Original Article | Neuroimaging and Head & Neck

eISSN 2005-8330
https://doi.org/10.3348/kjr.2020.0016
Korean J Radiol 2021;22(1):118-130

Korean Journal of Radiology
KJR

Blood-Brain Barrier Disruption in Mild Traumatic Brain Injury Patients with Post-Concussion Syndrome: Evaluation with Region-Based Quantification of Dynamic Contrast-Enhanced MR Imaging Parameters Using Automatic Whole-Brain Segmentation

Heera Yoen, MD[1], Roh-Eul Yoo, MD[1], Seung Hong Choi, MD[1, 2, 3], Eunkyung Kim, MD[4], Byung-Mo Oh, MD, PhD[4, 5, 6, 7], Dongjin Yang, MD[1], Inpyeong Hwang, MD[1], Koung Mi Kang, MD[1], Tae Jin Yun, MD[1], Ji-hoon Kim, MD[1], Chul-Ho Sohn, MD[1]

Departments of [1]Radiology and [4]Rehabilitation Medicine, Seoul National University Hospital, Seoul National University College of Medicine, Seoul, Korea; [2]Center for Nanoparticle Research, Institute for Basic Science (IBS), Seoul National University, Seoul, Korea; [3]School of Chemical and Biological Engineering, Seoul National University, Seoul, Korea; [5]Department of Rehabilitation Medicine, Seoul National University College of Medicine, Seoul, Korea; [6]National Traffic Injury Rehabilitation Hospital, Yangpyeong, Korea; [7]Neuroscience Research Institute, Seoul National University College of Medicine, Seoul, Korea

Objective: This study aimed to investigate the blood-brain barrier (BBB) disruption in mild traumatic brain injury (mTBI) patients with post-concussion syndrome (PCS) using dynamic contrast-enhanced (DCE) magnetic resonance (MR) imaging and automatic whole brain segmentation.

Materials and Methods: Forty-two consecutive mTBI patients with PCS who had undergone post-traumatic MR imaging, including DCE MR imaging, between October 2016 and April 2018, and 29 controls with DCE MR imaging were included in this retrospective study. After performing three-dimensional T1-based brain segmentation with FreeSurfer software (Laboratory for Computational Neuroimaging), the mean K^{trans} and v_p from DCE MR imaging (derived using the Patlak model and extended Tofts and Kermode model) were analyzed in the bilateral cerebral/cerebellar cortex, bilateral cerebral/cerebellar white matter (WM), and brainstem. K^{trans} values of the mTBI patients and controls were calculated using both models to identify the model that better reflected the increased permeability owing to mTBI (tendency toward higher K^{trans} values in mTBI patients than in controls). The Mann-Whitney U test and Spearman rank correlation test were performed to compare the mean K^{trans} and v_p between the two groups and correlate K^{trans} and v_p with neuropsychological tests for mTBI patients.

Results: Increased permeability owing to mTBI was observed in the Patlak model but not in the extended Tofts and Kermode model. In the Patlak model, the mean K^{trans} in the bilateral cerebral cortex was significantly higher in mTBI patients than in controls ($p = 0.042$). The mean v_p values in the bilateral cerebellar WM and brainstem were significantly lower in mTBI patients than in controls ($p = 0.009$ and $p = 0.011$, respectively). The mean K^{trans} of the bilateral cerebral cortex was significantly higher in patients with atypical performance in the auditory continuous performance test (commission errors) than in average or good performers ($p = 0.041$).

Conclusion: BBB disruption, as reflected by the increased K^{trans} and decreased v_p values from the Patlak model, was observed throughout the bilateral cerebral cortex, bilateral cerebellar WM, and brainstem in mTBI patients with PCS.

Keywords: *Blood-brain barrier; Magnetic resonance imaging; Perfusion; Permeability; Post-concussion syndrome*

Received: January 7, 2020 **Revised:** May 5, 2020 **Accepted:** May 24, 2020

This study was funded by Basic Science Research Program through the National Research Foundation of Korea (NRF) by the Ministry of Education (2017R1D1A1B04034838).

Corresponding author: Roh-Eul Yoo, MD, Department of Radiology, Seoul National University College of Medicine, 101 Daehak-ro, Jongno-gu, Seoul 03080, Korea.
• E-mail: roheul7@gmail.com

Korean Journal of Radiology
KJR

INTRODUCTION

Post-concussion syndrome (PCS) following mild traumatic brain injury (mTBI) is a major health and socioeconomic burden worldwide, especially in developed countries (1). Specifically, among 1.7 million people per year who visited hospitals in the United States for traumatic brain injury (TBI), an estimated 75% or more had mild injuries, according to the 2007 Centers for Disease Control and Prevention report (2, 3). Despite the high incidence and clinical importance of mTBI, the role of imaging has been neglected in the evaluation of mTBI than in moderate TBI or TBI of greater severity (3, 4). One of the reasons for this is the lack of a standardized and optimal imaging modality to evaluate mTBI accurately.

Over the past few years, there have been several attempts to evaluate mTBI noninvasively using various MR sequences, most of which were based on susceptibility-weighted imaging (SWI) (5-8) and diffusion tensor imaging (DTI) (9-11) for detecting microhemorrhages and fiber tract injuries, respectively. In line with these attempts, dynamic contrast-enhanced (DCE) MR imaging, an advanced MR imaging technique that can quantify the extent of blood-brain barrier (BBB) disruption in various central nervous system diseases through pharmacokinetic modeling (12-16), has been highlighted as a potentially useful tool to evaluate mTBI in several preclinical studies (17-19).

Moreover, the potential clinical utility of DCE MR imaging has also been investigated in mTBI patients with PCS, as conventional MR imaging performed in case of persistent PCS symptoms often fails to reveal any abnormality, causing frustration to both clinicians and patients in routine practice. A previous study on football players with histories of concussion revealed BBB dysfunction in various cortical regions (20). Furthermore, a more recent study on mTBI patients with PCS demonstrated that DCE MR imaging parameters, based on a two-compartment pharmacokinetic model proposed by Tofts and Kermode (12, 21, 22), significantly differed between mTBI patients and controls in certain manually defined regions-of-interest (ROIs) (23), implying that BBB disruption may have an important role in the pathophysiology of PCS in mTBI patients. However, given that manual ROI placement can be subjective, and subtle BBB disruption may be better reflected by the Patlak model (12, 21, 22), the potential clinical utility of DCE MR imaging in mTBI patients with PCS, as demonstrated by the previous study (23), remains elusive.

Therefore, this study aimed to further investigate BBB disruption in mTBI patients with PCS using DCE MR imaging and automatic whole-brain segmentation.

MATERIALS AND METHODS

This retrospective study was approved by the Institutional Review Board of our hospital, and the need for informed consent was waived.

Patient Selection

Based on our radiology report database between October 2016 and April 2018, 45 consecutive patients were identified under the following inclusion criteria: 1) patients with a clinical diagnosis of mTBI based on loss of consciousness not exceeding more than 0–30 minutes, posttraumatic amnesia or alteration of consciousness for less than 24 hours (24), 2) patients with a clinical diagnosis of PCS as defined by the International Classification of Diseases, 10th Revision (25), and 3) patients with contrast-enhanced MR imaging, including DCE MR imaging. Clinical diagnoses of mTBI and PCS were arrived at after history taking and neuropsychological examinations (Rivermead Post-concussion symptoms Questionnaire, RPQ [n = 30] and computerized neurocognitive function tests, CNTs [n = 26]) by the rehabilitation physician, blinded to the results of the DCE MR imaging (26-28) (Supplementary Table 1 for specific PCS symptoms in mTBI patients. Details for RPQ and CNTs are provided in Supplementary Materials). Exclusion criteria were as follows: 1) patients with severe structural abnormalities, including overt traumatic hemorrhage (n = 2), or 2) failure of automatic brain segmentation (n = 1) (Fig. 1).

For control subjects, 35 patients, who had undergone brain MR imaging, including DCE MR imaging, between November 2016 and March 2018, were identified under the following inclusion criteria: 1) patients with various neurological symptoms (headache [n = 25], mild memory impairment [n = 2], visual disturbance [n = 1], and dizziness [n = 1]), 2) patients with contrast-enhanced MR imaging, including DCE MR imaging, 3) patients with normal findings on conventional MR imaging, except for a few T2 hyperintensities not exceeding the age threshold (24), and 4) patients with no prior trauma history. Six patients were excluded owing to failure of automatic brain segmentation (Fig. 1).

Finally, 71 study subjects (42 patients and 29 controls) were included in this study. We reviewed the medical records of the mTBI patients and controls for the presence

 https://doi.org/10.3348/kjr.2020.0016

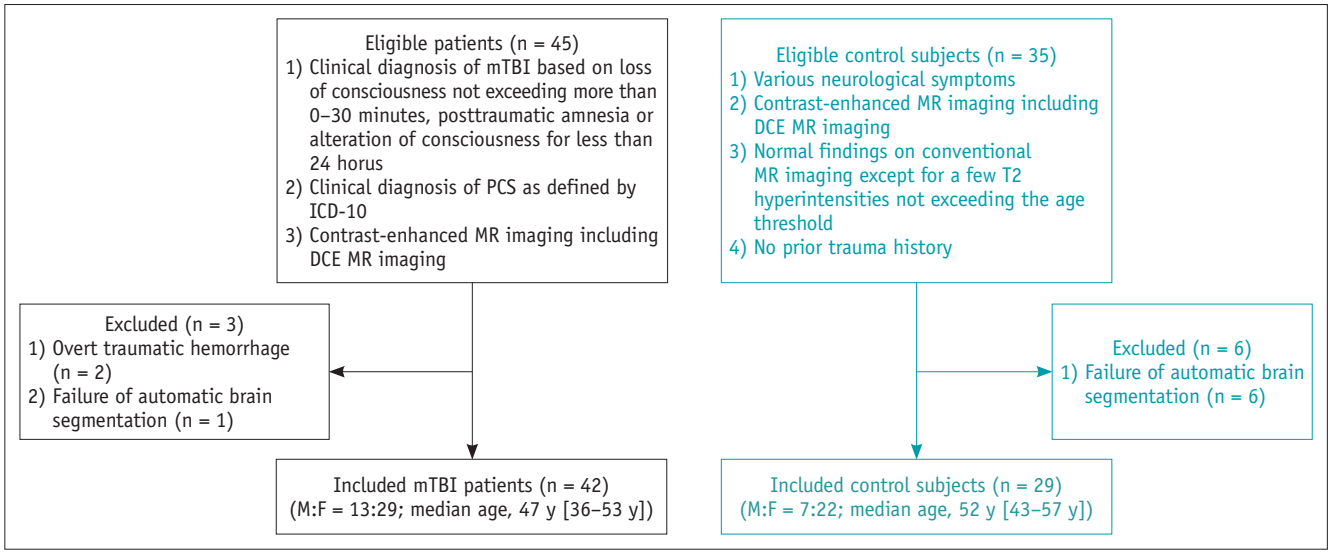

Fig. 1. Flowchart for selecting the study population. DCE = dynamic contrast-enhanced, ICD-10 = International Classification of Diseases, 10th Revision, mTBI = mild traumatic brain injury, PCS = post-concussion syndrome

of various comorbidities, such as diabetes, hypertension, dyslipidemia, chronic kidney disease, cerebral amyloid angiopathy, smoking history, and coronary artery disease.

Automatic Brain Segmentation and DCE MR Imaging Analysis

All MR images were acquired with a 3T scanner (Discovery 750, GE Healthcare) using a 32-channel head coil. The MR sequences included pre- and post-contrast three-dimensional (3D) fast spoiled gradient-echo (FSPGR), T2 fluid-attenuated inversion recovery (3D CUBE), diffusion-weighted imaging, SWI, and DCE MR imaging. For the DCE sequence, 3D fat-suppressed FSPGR imaging was obtained after intravenous administration of gadobutrol (at a dose of 0.1 mmol/kg of body weight), followed by a 30 mL saline bolus, at a rate of 4 mL/s using a power injector (Spectris, MedRad). Forty images were obtained at intervals equal to the repetition time for each section, resulting in a total acquisition time of 5 minutes and 8 seconds. Specific DCE MR imaging parameters were as follows: repetition time, 3 msec; echo time, 1.1 msec; flip angle, 10°; field of view, 240 x 240; matrix, 128 x 128; section thickness, 3 mm; and number of signals acquired, 0.7 (imaging parameters for other MR sequences are provided in Supplementary Table 2).

Based on the pre-contrast 3D T1-weighted images, automatic cortical reconstruction and volumetric whole-brain segmentation were performed using open-source software (FreeSurfer, version 6.0, Laboratory for Computational Neuroimaging). Using a dedicated commercial software package (NordicICE, version 4.1.2, NordicNeuroLab), K^{trans} and v_p maps were derived based on two pharmacokinetic models (the Patlak model and extended Tofts and Kermode model) by two reviewers (with 3 and 9 years of experience in neuroradiology, respectively), blinded to the results of neuropsychological tests, according to previously described methods (13, 23). Specifically, DCE MR imaging parameters were obtained using the arterial input function (AIF), which was semiautomatically derived from the main intracranial arteries, including the middle cerebral arteries at the level of the circle of Willis. This process was performed with the consensus of two radiologists (with 3 and 9 years of experience in neuroradiology, respectively). The final AIF curve was obtained using the cluster analysis technique. Subsequently, brain masks at five different regions (i.e., bilateral cerebral cortex and white matter [WM], bilateral cerebellar cortex and WM, and brainstem) were extracted (Fig. 2) and automatically co-registered with the K^{trans} and v_p maps to estimate mean K^{trans} and v_p values of these regions. Of note, K^{trans} values of the mTBI patients and controls were calculated using both models to identify the model that better reflected the increased permeability owing to mTBI (tendency toward higher K^{trans} values in mTBI patients than in controls).

Statistical Analysis

The normality of the parameters was assessed using the Kolmogorov-Smirnov test. The Wilcoxon signed-rank test was used to compare the mean K^{trans} values between the

https://doi.org/10.3348/kjr.2020.0016

Korean Journal of Radiology
KJR

Patlak model and extended Tofts and Kermode model. The Student's *t* test (or Mann-Whitney U test) was subsequently performed to compare DCE MR imaging parameters and noncategorical clinical variables between mTBI patients and controls. Subgroup analysis was performed according to the time interval between injury and MR imaging (three

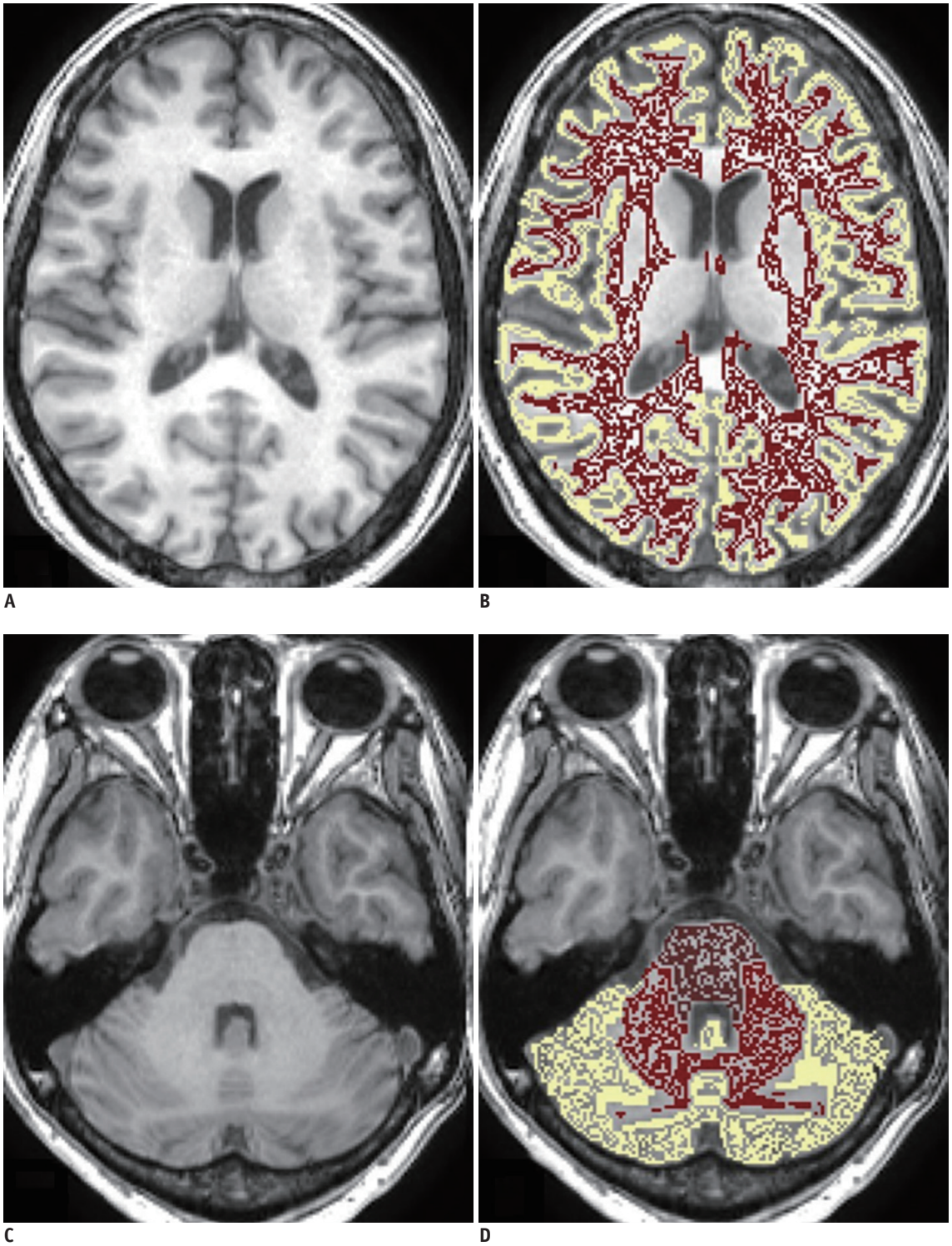

Fig. 2. Automatic brain segmentation and ROI mask extraction.
Based on precontrast three-dimensional T1-weighted images **(A, C)**, automatic cortical reconstruction and volumetric whole-brain segmentation were performed, and brain masks at bilateral cerebral cortex (yellow, **B**), bilateral cerebral WM (red, **B**), bilateral cerebellar cortex (yellow, **D**), bilateral cerebellar WM (red, **D**), and brainstem (brown, **D**) were extracted afterward. ROI = region-of-interest, WM = white matter

https://doi.org/10.3348/kjr.2020.0016

months or less vs. longer than three months) to compare the DCE MR imaging parameters between the two groups. Categorical clinical variables were compared between the two groups using Fisher's exact test. Pearson correlation analysis or Spearman's rank correlation test was used, as appropriate, to identify the correlations between the DCE MR imaging parameters and clinical parameters, including the time interval between the injury and MR imaging and neuropsychological test scores. Specifically, we assessed the correlation between DCE MR imaging parameters and neuropsychological test scores only for the subgroup of patients with a time interval of ≤ 2 weeks between the neuropsychological tests and MR scanning. The DCE MR imaging parameters of patients with average or good performance in CNTs were further compared to those with moderately or markedly atypical performance using the Mann-Whitney U-test. Receiver operating characteristic (ROC) curves were obtained to evaluate the diagnostic performance of the DCE MR imaging parameters and their optimal threshold values to discriminate between patients with average or good performance in CNTs and those with moderately or markedly atypical performance. Intraclass correlation coefficients (ICC) were calculated to evaluate interobserver agreements for DCE MR imaging parameters. All statistical analyses were performed using MedCalc, version 11.1.1.0 (MedCalc) and SPSS Statistics for Windows, Version 23.0 (IBM Corp.). A *p* value of less than 0.05 was considered statistically significant.

RESULTS

Demographic and Conventional MR Findings of mTBI Patients and Controls

Age did not significantly differ between mTBI patients {median, 47 years (interquartile range [IQR], 36–53 years)} and controls (median, 52 years [IQR, 43–57 years]) (p = 0.064). No statistically significant difference in sex was found between the two groups (p = 0.177). In addition, there was no significant difference in the incidence of comorbidities between these two groups (11.9% [5/42] vs. 6.9% [2/29]; p = 0.692) (Table 1).

Among the 71 study subjects, including mTBI patients, none showed discernable trauma-related findings, such as intracranial hemorrhage or fracture on conventional MR sequences. However, most of the patients (69.0% [29/42] of the mTBI group, 58.6% [17/29] of the control group) had a few foci with T2 high signal intensity scattered in the cerebral WM not exceeding the age threshold (p = 0.451).

DCE MR Imaging Analysis

Comparison of Mean K^{trans} according to Pharmacokinetic Models

Table 2 shows the mean K^{trans} values based on two

Table 1. Clinical Characteristics of mTBI Patients and Controls

Characteristics	mTBI (n = 42)	Controls (n = 29)	*P*
Age (y)*	47 (36–53)	52 (43–57)	0.064
Sex			0.599
Male	13 (31.0)	7 (24.1)	
Female	29 (69.0)	22 (75.9)	
Time interval between injury and MR imaging (months)*	2.0 (1.0–5.0)	NA	NA
Time interval between MR imaging and neuropsychological tests (weeks)*			
RPQ (n = 30)	1.7 (0.8–3.3)	NA	NA
CNT (n = 26)	0.7 (0–1.7)	NA	NA
Comorbidity	5 (11.9)	2 (6.9)	0.692
Diabetes mellitus	0 (0)	1 (3.4)	0.408
Hypertension	2 (4.8)	0 (0)	0.510
Dyslipidemia	3 (7.1)	1 (3.4)	0.640
Chronic kidney disease	0 (0)	0 (0)	NA
Cerebral amyloid angiopathy	0 (0)	0 (0)	NA
Smoking	0 (0)	0 (0)	NA
Coronary artery disease	0 (0)	0 (0)	NA

Unless otherwise indicated, data represent the number of patients. Data in the parentheses are percentages. *Data are reported as medians (interquartile range). CNT = computerized neurocognitive function test, mTBI = mild traumatic brain injury, RPQ = Rivermead Post-concussion symptoms Questionnaire, NA = not available

https://doi.org/10.3348/kjr.2020.0016

Korean Journal of Radiology
KJR

Table 2. Mean K^{trans} according to Pharmacokinetic Models

Brain Regions	mTBI (n = 42)			Controls (n = 29)		
	Patlak	Extended TK	*P*	Patlak	Extended TK	*P*
Bilateral cerebral cortex ($\times 10^{-1}$ min^{-1})	0.0104 (0.0084–0.0135)	0.1389 (0.1015–0.1815)	< 0.001	0.0084 (0.0072–0.0119)	0.1452 (0.1243–0.1697)	< 0.001
Bilateral cerebral WM ($\times 10^{-1}$ min^{-1})	0.0036 (0.0028–0.0046)	0.0468 (0.0397–0.0649)	< 0.001	0.0031 (0.0027–0.0041)	0.0470 (0.0414–0.0559)	< 0.001
Bilateral cerebellar cortex ($\times 10^{-1}$ min^{-1})	0.0081 (0.0062–0.0112)	0.1131 (0.0875–0.1558)	< 0.001	0.0074 (0.0056–0.0089)	0.1380 (0.1036–0.1656)	< 0.001
Bilateral cerebellar WM ($\times 10^{-1}$ min^{-1})	0.0041 (0.0033–0.0049)	0.0568 (0.0425–0.0799)	< 0.001	0.0038 (0.0027–0.0043)	0.0659 (0.0555–0.0824)	< 0.001
Brainstem ($\times 10^{-1}$ min^{-1})	0.0052 (0.0044–0.0062)	0.0660 (0.0515–0.0961)	< 0.001	0.0052 (0.0043–0.0066)	0.0856 (0.0657–0.1021)	< 0.001

Data represent medians (interquartile range) unless otherwise noted. Extended TK = extended Tofts and Kermode model, WM = white matter

different pharmacokinetic models in the mTBI and control groups. The mean K^{trans} values based on the Patlak model were significantly lower than those based on the extended Tofts and Kermode model at all five locations ($p < 0.001$). Increased permeability owing to mTBI was observed in the Patlak model, but not in the extended Tofts and Kermode model (Fig. 3).

Comparison of DCE MR Imaging Parameters (from the Patlak Model) between mTBI Patients and Controls

All patients showed symmetrical perfusion on the visual assessment of both K^{trans} and v_p maps. However, the mean K^{trans} value of the bilateral cerebral cortex was significantly higher in mTBI patients (median, 0.0104 x 10^{-1} min^{-1} [IQR, 0.0084–0.0135 x 10^{-1} min^{-1}]) than in controls (median, 0.0084 x 10^{-1} min^{-1} [IQR, 0.0072–0.0119 x 10^{-1} min^{-1}]) ($p = 0.042$) (Table 2, Figs. 4, 5). Meanwhile, the mean v_p values of the bilateral cerebellar WM and brainstem were significantly lower in mTBI patients than in controls (bilateral cerebellar WM: median, 0.85 [IQR, 0.73–0.99] vs. median, 1.00 [IQR, 0.84–1.16], $p = 0.009$; brainstem: median, 1.15 [IQR, 1.01–1.43] vs. median, 1.40 [IQR, 1.13–1.64], $p = 0.011$) (Table 3, Figs. 4, 6).

Correlations between DCE MR Imaging Parameters (from the Patlak Model) and Time Interval between Injury and MR Imaging

DCE MR imaging parameters (i.e., the mean K^{trans} of the bilateral cerebral cortex, v_p of the bilateral cerebellar WM, and v_p of the brainstem) were not significantly correlated with the time interval between injury and MR imaging ($\rho = 0.028$, $p = 0.858$; $\rho = -0.090$, $p = 0.571$; $\rho = -0.081$, $p = 0.612$; respectively).

In the subgroup analysis according to the time interval between injury and MR imaging (three months or less vs. longer than three months), the mean K^{trans} values of the bilateral cerebral cortex of both subgroups tended to be higher than those of controls, although the difference was not statistically significant (for three months or less, $p = 0.093$; for longer than three months, $p = 0.077$) (Supplementary Table 3).

The mean v_p values of the bilateral cerebellar WM of both subgroups were significantly lower than those of controls (for three months or less, $p = 0.047$; for longer than three months, $p = 0.012$). The mean v_p values of the brainstem of both subgroups tended to be lower than those of controls, although the statistical significance was only achieved for the subgroup with the interval longer than three months (for three months or less, $p = 0.086$; for longer than three months, $p = 0.008$) (Supplementary Table 3).

Correlation between DCE MR Imaging Parameters (from the Patlak Model) and Neuropsychological Tests

Detailed scores for all RPQ (n = 30) and CNTs (n = 26) are summarized in Table 4. Among those, 18 patients and 19 patients had imaging-neuropsychological test time intervals of two weeks or less for RPQ and CNTs, respectively. In this subgroup of patients, no significant correlation was found between DCE MR imaging parameters and neuropsychological test scores (all $p > 0.05$) (Fig. 7). However, the mean K^{trans} value of the bilateral cerebral cortex was significantly higher in patients with atypical performance in the auditory continuous performance test (commission errors) (median, 0.0122 x 10^{-1} min^{-1} [IQR, 0.0096–0.0165 x 10^{-1} min^{-1}]) than

 https://doi.org/10.3348/kjr.2020.0016

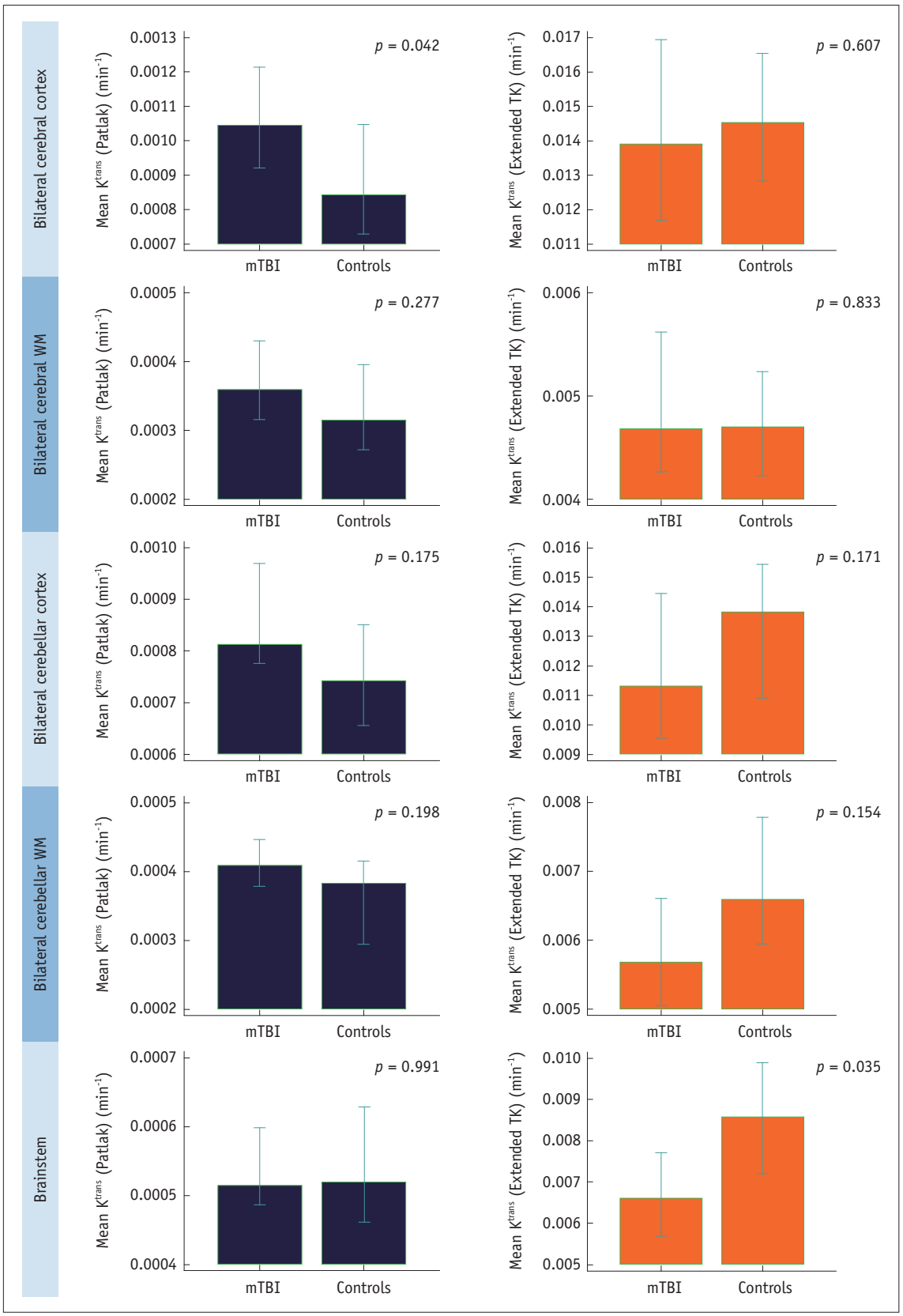

Fig. 3. Bar graphs show mean K^{trans} values according to pharmacokinetic models. A tendency toward higher K^{trans} values in mTBI patients than in controls was observed in the Patlak model but not in the Extended TK. Each error bar depicts the 95% confidence interval for the median. Extended TK = extended Tofts and Kermode model

https://doi.org/10.3348/kjr.2020.0016

Korean Journal of Radiology
KJR

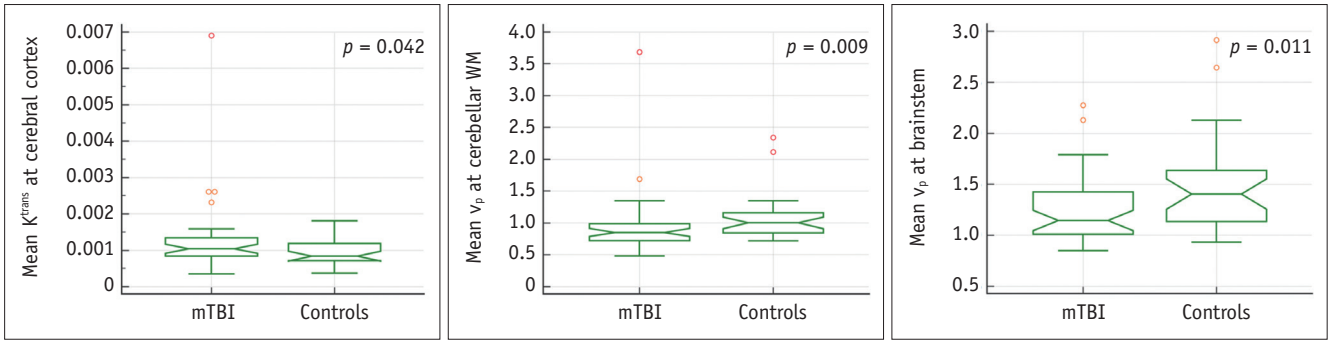

Fig. 4. Notched box-and-whisker plots for DCE MR imaging parameters at bilateral cerebral cortex, bilateral cerebellar WM, and brainstem. Notched lines of boxes represent median values, while boundaries of the box show the first and third interquartile values. Lower and upper ends of the plots denote the minimal and maximal values and outliers beyond this range are displayed individually.
A. Mean K^{trans} value in bilateral cerebral cortex was significantly higher in mTBI patients (median, 0.0104 x 10^{-1} min^{-1}) than in controls (median, 0.0084 x 10^{-1} min^{-1}). **B, C.** mTBI patients had significantly lower mean v_p values at bilateral cerebellar WM and brainstem (0.85 and 1.15, respectively) than controls (1.00 and 1.40, respectively).

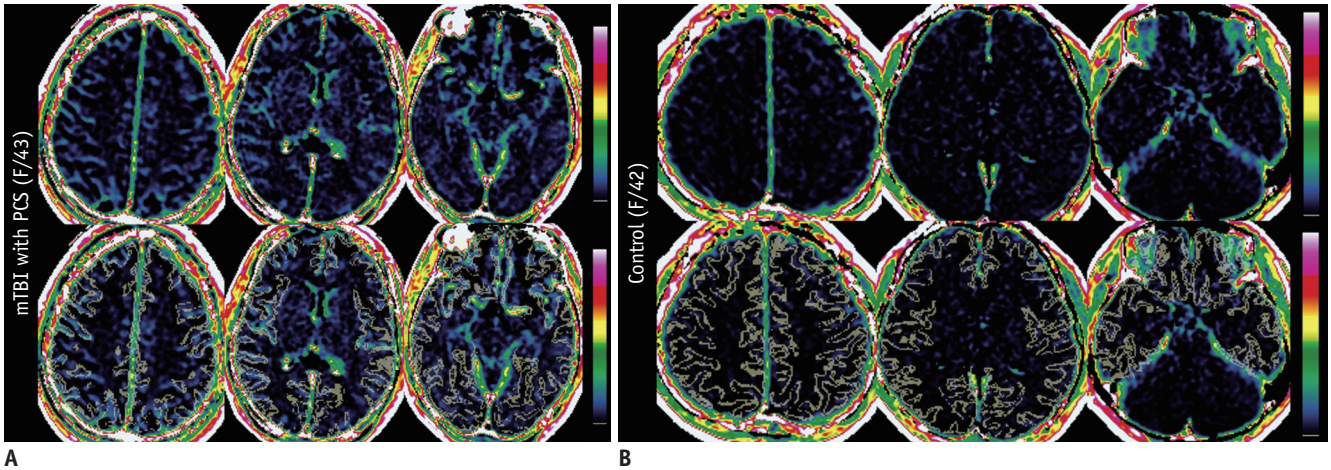

Fig. 5. Representative K^{trans} maps before and after co-registration with ROI masks for bilateral cerebral cortex in a 43-year-old mTBI female patient (A) and a 42-year-old female control (B). (**A, B;** upper rows) K^{trans} maps before co-registration demonstrate apparently higher K^{trans} values in the mTBI patient than in the control throughout bilateral cerebral cortex. (**A, B;** lower rows) Mean K^{trans} values measured from the co-registered K^{trans} maps were 0.0261 x 10^{-1} min^{-1} for the mTBI patient and 0.0045 x 10^{-1} min^{-1} for the control.

in those with average or good performance (median, 0.0089 x 10^{-1} min^{-1} [IQR, 0.0080–0.0111 x 10^{-1} min^{-1}]) (p = 0.041). In the ROC analysis, the mean K^{trans} value of the bilateral cerebral cortex had a sensitivity of 70.0% and a specificity of 88.9% for differentiating the patients with atypical performance and those with average or good performance at a cut-off value of 0.0093 x 10^{-1} min^{-1}.

Interobserver Agreement for Quantitative DCE MR Imaging Parameters (from the Patlak Model)

The ICC value for interobserver agreement was almost perfect (K^{trans} value, 0.916 [95% confidence interval, CI]: 0.899–0.930; v_p value, 0.988 [95% CI]: 0.985–0.991) between the two observers.

DISCUSSION

BBB disruption has received increased attention as one of the major pathophysiologies underlying TBI, based on the results of previous studies that assessed BBB disruption in animal models using Evans blue staining (21) or immunohistochemistry for serum proteins (29). In parallel with the growing evidence from histopathological data, DCE MR imaging has been highlighted as a promising imaging counterpart for the noninvasive evaluation of BBB injury in TBI animal models (21, 30) and humans (20, 23). To our knowledge, this study is one of the few clinical studies applying DCE MR imaging on mTBI patients. Unlike previous studies (20, 31), we applied automatic segmentation and

https://doi.org/10.3348/kjr.2020.0016

Table 3. Comparison of DCE MR Imaging Parameters (from the Patlak Model) between mTBI Patients and Controls

Brain Regions	mTBI (n = 42)	Controls (n = 29)	*P*
Bilateral cerebral cortex			
Mean K^{trans} (x 10^{-1} min^{-1})	0.0104 (0.0084–0.0135)	0.0084 (0.0072–0.0119)	0.042
Mean v_p	1.93 (1.71–2.25)	1.98 (1.80–2.35)	0.433
Bilateral cerebral WM			
Mean K^{trans} (x 10^{-1} min^{-1})	0.0036 (0.0028–0.0046)	0.0031 (0.0027–0.0041)	0.277
Mean v_p	0.76 (0.64–0.85)	0.75 (0.66–0.90)	0.575
Bilateral cerebellar cortex			
Mean K^{trans} (x 10^{-1} min^{-1})	0.0081 (0.0062–0.0112)	0.0074 (0.0056–0.0089)	0.175
Mean v_p	1.50 (1.34–1.81)	1.70 (1.48–2.13)	0.107
Bilateral cerebellar WM			
Mean K^{trans} (x 10^{-1} min^{-1})	0.0041 (0.0033–0.0049)	0.0038 (0.0027–0.0043)	0.198
Mean v_p	0.85 (0.73–0.99)	1.00 (0.84–1.16)	0.009
Brainstem			
Mean K^{trans} (x 10^{-1} min^{-1})	0.0052 (0.0044–0.0062)	0.0052 (0.0043–0.0066)	0.991
Mean v_p	1.15 (1.01–1.43)	1.40 (1.13–1.64)	0.011

Data represent medians (interquartile range) unless otherwise noted. All the DCE parameters were derived using the Patlak model. DCE = dynamic contrast-enhanced

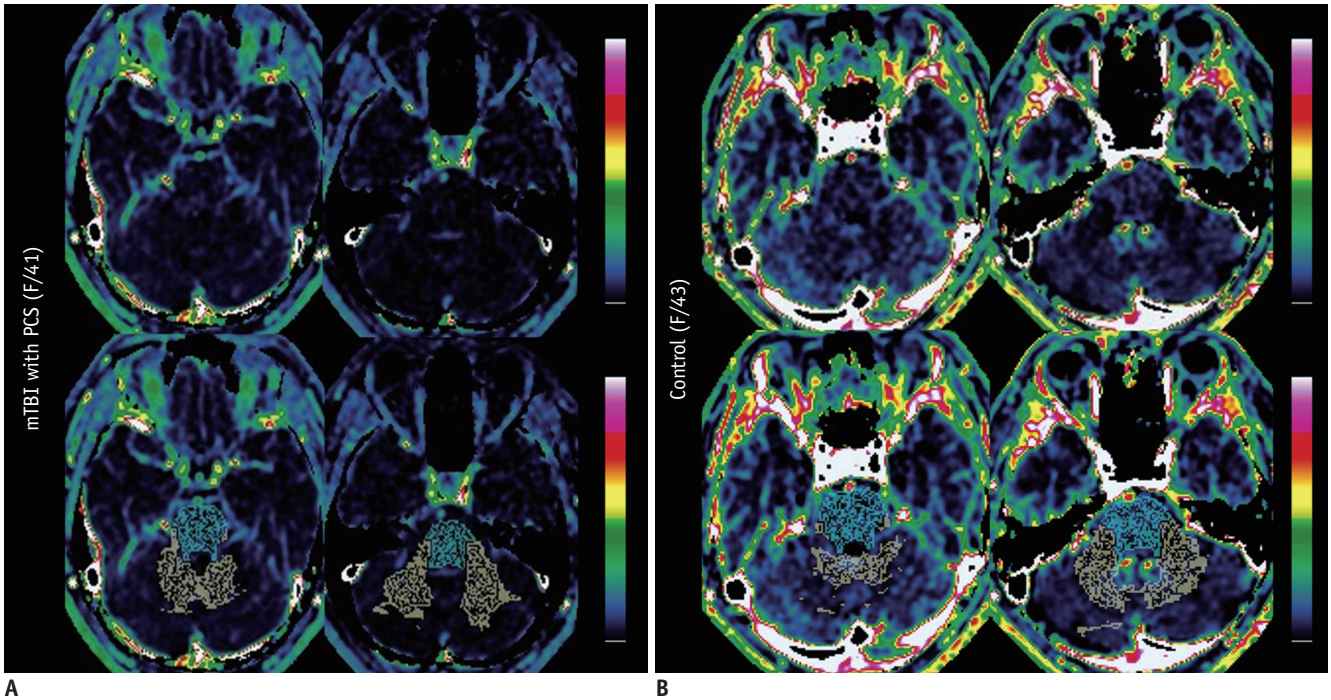

A B

Fig. 6. Representative v_p maps before and after co-registration with ROI masks for bilateral cerebellar WM and brainstem in a 41-year-old mTBI female patient (A) and a 43-year-old female control (B). (**A, B;** upper rows) v_p maps before co-registration depict apparently lower v_p values in the mTBI patient than in the control throughout the cerebellar WM and brainstem. (**A, B;** lower rows) Mean v_p values in bilateral cerebellar WM measured from the co-registered v_p maps were 0.48 for the mTBI patient and 1.16 for the control, while mean v_p values in the brainstem were 0.85 for the mTBI patient and 1.44 for the control.

two different pharmacokinetic models (the Patlak model and extended Tofts and Kermode model) for a more rigorous analysis of the subtle alteration of BBB permeability in mTBI. We found that the K^{trans} value of the cerebral cortex was significantly higher in mTBI patients compared to the controls. Meanwhile, the v_p values of the cerebellar WM and brainstem were lower in the patients than in the controls. Furthermore, the K^{trans} value of the cerebral cortex was significantly higher for poor performers on the auditory continuous performance test (commission errors).

https://doi.org/10.3348/kjr.2020.0016

Korean Journal of Radiology
KJR

In DCE MR imaging, contrast media composed of low-molecular gadolinium reach the brain tissue and distribute between the blood plasma and extravascular extracellular space (EES) through the BBB, which acts as a filter. Under the circumstances of BBB injury following trauma, gadolinium distribution across the BBB differs from that in normal brain tissue. This difference in gadolinium distribution owing to the change in BBB permeability can be calculated based on a DCE MR pharmacokinetic model and represented by quantitative variables, such as K^{trans} (i.e., volume transfer constant between the plasma and EES), v_p (i.e., fractional plasma volume), and v_e (i.e., fractional interstitial volume). There are several pharmacokinetic models in use, with the conventional Tofts model, extended Tofts model, and Patlak model being the most popular (12, 21, 22). Both the extended Tofts model and the Patlak model can be used for highly perfused tissue. However, unlike the extended Tofts model, which considers bidirectional transport, including back-diffusion from the EES into plasma, the Patlak model ignores this back-diffusion and therefore provides estimates for only two parameters (K^{trans} and v_p). Because of the additional complexity of the extended Tofts model in considering back-diffusion, which may cause over-fitting in low-permeability settings, the Patlak model is reported to be more accurate for measuring normal and slightly increased permeability with negligible back-diffusion (12, 21, 32). Although we found measured K^{trans} values to be significantly higher on the extended Tofts and Kermode model than in the Patlak model, our results demonstrated that the Patlak model might be more suitable for reflecting the difference between mTBI patients with low permeability and controls, in keeping with the previous findings.

Based on DCE imaging parameters obtained using the Patlak model, we demonstrated that the BBB permeability of the cerebral cortex was significantly different between mTBI patients and controls, in keeping with a previous study that reported BBB lesions in various cortical regions in football players with histories of concussion (20). Several studies have demonstrated cortical involvement in mTBI patients. Specifically, in brain contusions, which are one of

Table 4. Scores of RPQ and Neurocognitive Function Tests

Tests	Scores
RPQ* (n = 30)	34.0 (27.0–45.0)
RPQ-3	6.5 (5.0–9.0)
RPQ-13	27.0 (21.0–37.0)
CNT (n = 26)	
Auditory CPT (correct responses)†	40.0 (27.0–49.0)
Auditory CPT (commission errors)†	45.0 (27.0–62.0)
VLT (immediate recall)†	52.5 (45.0–59.0)
VLT (delayed recall)†	50.0 (42.0–70.0)
VLT (delayed recognition)†	46.5 (36.0–57.0)
Digit span test (forward)†	43.0 (35.0–46.0)
Digit span test (backward)†	50.0 (38.0–53.0)
Card sorting test (perseverative response)†	51.5 (46.0–64.0)

Data are reported as the median (interquartile range). *The total RPQ score for 16 PCS symptoms ranges from 0 to 64 with a higher score representing a greater degree of symptoms. The test is composed of RPQ-3 (3 items for scoring headaches, nausea and/or vomiting, and dizziness, representing early concussion symptoms) and RPQ-13 (13 items for scoring cognitive, mood, sleep, and other physical symptoms, indicative of later symptoms of PCS) (26), †T scores. CPT = continuous performance test, PCS = post-concussion syndrome, VLT = verbal learning test

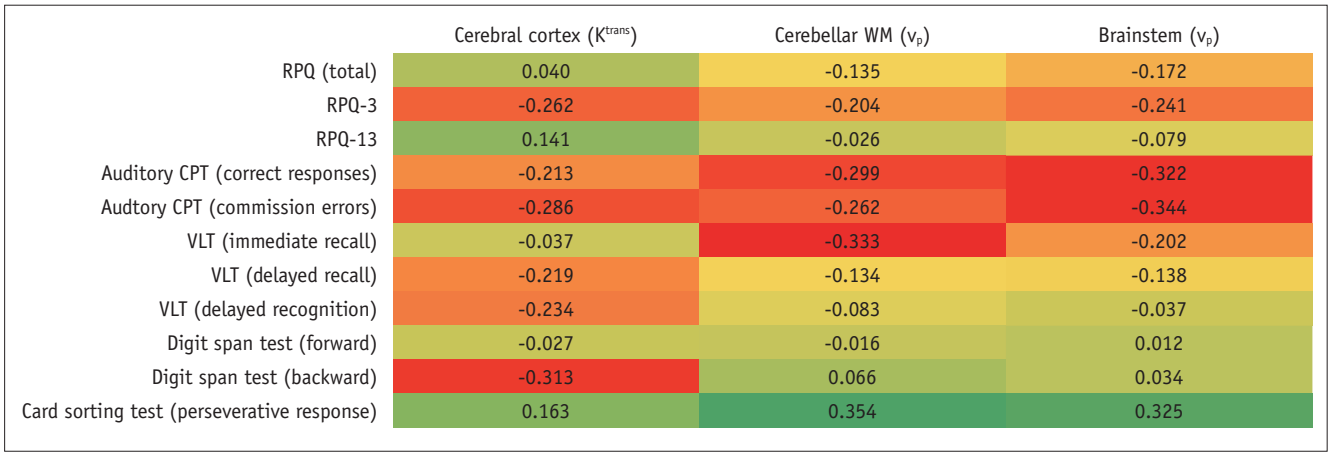

Fig. 7. A heatmap for the Spearman correlation analysis between DCE MR imaging parameters and neuropsychological tests.
No significant correlation was found between DCE MR imaging parameters and neuropsychological test scores (all $p > 0.05$). CPT = continuous performance test, RPQ = Rivermead Post-concussion symptoms Questionnaire, VLT = verbal learning test

https://doi.org/10.3348/kjr.2020.0016

the structural abnormalities found in mTBI, collision between soft brain parenchyma and the surrounding rigid bone usually affects the subpial cortical surface first and subsequently extends through the cortex with disruption of tissue and vessels or BBB (33, 34). A reduction in cortical thickness was also noted in ice hockey team members with PCS (35).

In addition to the cortical BBB abnormality, v_p values were found to be significantly lower in the cerebellar WM and brainstem. Although these regions are known to be more frequently affected in severe injury than in mild injury, diffuse neuronal and axonal injury has also been reported in mTBI patients, as evidenced by a global decrease of WM fractional anisotropy (including the brainstem and cerebellums) on DTI (36, 37) as well as a reduction in whole-brain N-acetylaspartate (38).

Our study results are similar to those of a previous study, which reported higher K^{trans} and v_e values at various regions (including T2 hyperintense WM lesions, normal-appearing WM, and predilection sites for diffuse axonal injury) in mTBI patients with PCS than in controls (23). However, we applied automatic whole-brain segmentation to select ROIs rather than manually defining the areas as in the previous study. Therefore, we believe that our results avoid the inherent subjectivity of manual ROI placement and provide more objective evidence for BBB disruption in mTBI patients. Moreover, it is noteworthy that a significant difference was observed in the K^{trans} value of the cerebral cortex between poor and good performers in the auditory continuous performance test (commission errors). Although the results are preliminary given the small sample size, the difference may indicate that DCE MR imaging parameters could be imaging biomarkers not only for the BBB injury itself but also for the severity of impairment in attention following mTBI.

Unlike the previous study, which reported high BBB permeability in the cerebral WM (20), we did not find a significant difference in permeability in the bilateral cerebral WM between mTBI patients with PCS and controls. The lack of statistically significant difference may be partially attributed to the use of mean values for the entire cerebral WM, which would lead to averaging the data from not only the site of traumatic impact but also the unaffected WM. We inevitably used the mean values because the coup sites were not obvious from either medical histories or MR images in our patients. Thus, further investigation in future studies, including patients with known coup sites, is warranted.

This study has several limitations apart from those of a retrospective study, including selection bias of the patient pool. First, some of the patients did not undergo neuropsychological tests, and thus, these cases were excluded from the subgroup analysis. In addition, we could not strictly control the time interval between MR imaging and neuropsychological tests, which further limited the study population for the subgroup analysis. These factors led to the small sample size, which could have partially contributed to the lack of significant association between DCE MR imaging parameters and neuropsychological test scores other than auditory continuous performance test (commission errors). However, it was inevitable, given the clinical feature of mTBI with PCS, which is characterized by fluctuating symptoms with variable onsets that do not require prompt medical management, limited resource availability (especially MR scanners), as well as the retrospective nature of the study. Therefore, a further prospective study with larger sample size is needed to validate the correlation. Second, the control group without TBI was not explicitly age- and sex-matched. Nevertheless, there were no significant differences in age and sex between mTBI patients and controls in the statistical analysis, with the median age being slightly younger in the patients. Considering that the aging process can also increase BBB permeability, higher permeability in mTBI patients despite the younger median age supports the significant influence of trauma on BBB permeability. The detected difference in permeability could have been even higher if age-matched controls had been included. Moreover, given that BBB permeability can be increased by numerous neurological diseases, such as primary headache (e.g., migraine) (13), the possibility remains that the inclusion of age-matched individuals without any neurological symptoms, as controls, could have resulted in even lower K^{trans} and higher v_p for the control group, which may further amplify the detected differences between the patients and controls. Third, caution is warranted when assessing DCE MR imaging parameters (especially v_p) because several factors, such as plasma perfusion, can also affect the absolute values of the parameters resulting in values exceeding the theoretical range (i.e., v_p higher than 1 in certain regions). Nonetheless, the observed tendency in permeability difference between the mTBI and control groups would still hold true because we applied the same model for these two groups. Fourth, we used mean values for the entire cerebral cortex rather than those for cortical

https://doi.org/10.3348/kjr.2020.0016

Korean Journal of Radiology
KJR

regions at the site of traumatic impact because the coup sites were not obvious from either medical histories or MR images in our patients. Therefore, the difference in BBB permeability between the mTBI with PCS group and controls could have been underestimated.

In conclusion, DCE MR imaging parameters derived from the Patlak model can depict subtle changes in BBB permeability in mTBI patients with PCS and therefore may have a complementary role in mTBI patients with otherwise normal conventional MR imaging findings. In particular, increased BBB permeability, as reflected by higher K^{trans} and lower v_p, values, was observed throughout the cerebral cortex, cerebellar WM, and brainstem in mTBI patients with PCS.

Supplementary Materials

The Data Supplement is available with this article at https://doi.org/10.3348/kjr.2020.0016.

Conflicts of Interest

The authors have no potential conflicts of interest to disclose.

ORCID iDs

Heera Yoen
https://orcid.org/0000-0001-5583-6065
Roh-Eul Yoo
https://orcid.org/0000-0002-5625-5921
Seung Hong Choi
https://orcid.org/0000-0002-0412-2270
Eunkyung Kim
https://orcid.org/0000-0001-6264-722X
Byung-Mo Oh
https://orcid.org/0000-0001-9353-7541
Dongjin Yang
https://orcid.org/0000-0003-1993-9053
Inpyeong Hwang
https://orcid.org/0000-0002-1291-8973
Koung Mi Kang
https://orcid.org/0000-0001-9643-2008
Tae Jin Yun
https://orcid.org/0000-0001-8441-4574
Ji-hoon Kim
https://orcid.org/0000-0002-6349-6950
Chul-Ho Sohn
https://orcid.org/0000-0003-0039-5746

REFERENCES

1. Shukla D, Devi BI. Mild traumatic brain injuries in adults. *J Neurosci Rural Pract* 2010;1:82-88
2. Coronado VG, Xu L, Basavaraju SV, McGuire LC, Wald MM, Faul M, et al. Surveillance for traumatic brain injury-related deaths--United States, 1997-2007. *MMWR Surveill Summ* 2011;60:1-32
3. McMahon PJ, Hricik A, Yue JK, Puccio AM, Inoue T, Lingsma HF, et al. Symptomatology and functional outcome in mild traumatic brain injury: results from the prospective TRACK-TBI study. *J Neurotrauma* 2014;31:26-33
4. Ruff R. Two decades of advances in understanding of mild traumatic brain injury. *J Head Trauma Rehabil* 2005;20:5-18
5. Liu G, Ghimire P, Pang H, Wu G, Shi H. Improved sensitivity of 3.0 tesla susceptibility-weighted imaging in detecting traumatic bleeds and its use in predicting outcomes in patients with mild traumatic brain injury. *Acta Radiol* 2015;56:1256-1263
6. Liu T, Surapaneni K, Lou M, Cheng L, Spincemaille P, Wang Y. Cerebral microbleeds: burden assessment by using quantitative susceptibility mapping. *Radiology* 2012;262:269-278
7. Liu W, Soderlund K, Senseney JS, Joy D, Yeh PH, Ollinger J, et al. Imaging cerebral microhemorrhages in military service members with chronic traumatic brain injury. *Radiology* 2016;278:536-545
8. Mittal S, Wu Z, Neelavalli J, Haacke EM. Susceptibility-weighted imaging: technical aspects and clinical applications, Part 2. *AJNR Am J Neuroradiol* 2009;30:232-252
9. Bouix S, Pasternak O, Rathi Y, Pelavin PE, Zafonte R, Shenton ME. Increased gray matter diffusion anisotropy in patients with persistent post-concussive symptoms following mild traumatic brain injury. *PLoS One* 2013;8:e66205
10. Fakhran S, Yaeger K, Collins M, Alhilali L. Sex differences in white matter abnormalities after mild traumatic brain injury: localization and correlation with outcome. *Radiology* 2014;272:815-823
11. Yuh EL, Cooper SR, Mukherjee P, Yue JK, Lingsma HF, Gordon WA, et al. Diffusion tensor imaging for outcome prediction in mild traumatic brain injury: a TRACK-TBI study. *J Neurotrauma* 2014;31:1457-1477
12. Cramer SP, Larsson HB. Accurate determination of blood-brain barrier permeability using dynamic contrast-enhanced T1-weighted MRI: a simulation and in vivo study on healthy subjects and multiple sclerosis patients. *J Cereb Blood Flow Metab* 2014;34:1655-1665
13. Kim YS, Kim M, Choi SH, You SH, Yoo RE, Kang KM, et al. Altered vascular permeability in migraine-associated brain regions: evaluation with dynamic contrast-enhanced MRI. *Radiology* 2019;292:713-720
14. Taheri S, Gasparovic C, Huisa BN, Adair JC, Edmonds E, Prestopnik J, et al. Blood-brain barrier permeability abnormalities in vascular cognitive impairment. *Stroke*

2011;42:2158-2163
15. Thornhill RE, Chen S, Rammo W, Mikulis DJ, Kassner A. Contrast-enhanced MR imaging in acute ischemic stroke: T2* measures of blood-brain barrier permeability and their relationship to T1 estimates and hemorrhagic transformation. *AJNR Am J Neuroradiol* 2010;31:1015-1022
16. Yun TJ, Park CK, Kim TM, Lee SH, Kim JH, Sohn CH, et al. Glioblastoma treated with concurrent radiation therapy and temozolomide chemotherapy: differentiation of true progression from pseudoprogression with quantitative dynamic contrast-enhanced MR imaging. *Radiology* 2015;274:830-840
17. Wei XE, Wang D, Li MH, Zhang YZ, Li YH, Li WB. A useful tool for the initial assessment of blood-brain barrier permeability after traumatic brain injury in rabbits: dynamic contrast-enhanced magnetic resonance imaging. *J Trauma* 2011;71:1645-1651
18. Li W, Watts L, Long J, Zhou W, Shen Q, Jiang Z, et al. Spatiotemporal changes in blood-brain barrier permeability, cerebral blood flow, T2 and diffusion following mild traumatic brain injury. *Brain Res* 2016;1646:53-61
19. Wei XE, Zhang YZ, Li YH, Li MH, Li WB. Dynamics of rabbit brain edema in focal lesion and perilesion area after traumatic brain injury: a MRI study. *J Neurotrauma* 2012;29:2413-2420
20. Weissberg I, Veksler R, Kamintsky L, Saar-Ashkenazy R, Milikovsky DZ, Shelef I, et al. Imaging blood-brain barrier dysfunction in football players. *JAMA Neurol* 2014;71:1453-1455
21. Heye AK, Culling RD, Valdés Hernández M del C, Thrippleton MJ, Wardlaw JM. Assessment of blood-brain barrier disruption using dynamic contrast-enhanced MRI. A systematic review. *Neuroimage Clin* 2014;6:262-274
22. Sourbron SP, Buckley DL. Classic models for dynamic contrast-enhanced MRI. *NMR Biomed* 2013;26:1004-1027
23. Yoo RE, Choi SH, Oh BM, Shin SD, Lee EJ, Shin DJ, et al. Quantitative dynamic contrast-enhanced MR imaging shows widespread blood-brain barrier disruption in mild traumatic brain injury patients with post-concussion syndrome. *Eur Radiol* 2019;29:1308-1317
24. Riedy G, Senseney JS, Liu W, Ollinger J, Sham E, Krapiva P, et al. Findings from structural MR imaging in military traumatic brain injury. *Radiology* 2016;279:207-215
25. World Health Organization. *ICD-10: international statistical classification of diseases and related health problems, tenth revision*, 2nd ed. Geneva: World Health Organization, 2004
26. King NS, Crawford S, Wenden FJ, Moss NE, Wade DT. The Rivermead Post concussion symptoms Questionnaire: a measure of symptoms commonly experienced after head injury and its reliability. *J Neurol* 1995;242:587-592
27. Lezak MD, Howieson DB, Loring DW, Hannay HJ, Fischer JS. *Neuropsychological assessment*, 4th Ed. New York: Oxford University Press, 2004
28. Kwon JS, Lyoo IK, Hong KS, Yeon BK, Ha KS. Development and standardization of the computerized memory assessment for Korean adults. *J Korean Neuropsychiatr Assoc* 2002;41:347-362
29. Johnson VE, Weber MT, Xiao R, Cullen DK, Meaney DF, Stewart W, et al. Mechanical disruption of the blood-brain barrier following experimental concussion. *Acta Neuropathol* 2018;135:711-726
30. Wang ML, Li WB. Cognitive impairment after traumatic brain injury: the role of MRI and possible pathological basis. *J Neurol Sci* 2016;370:244-250
31. Winter C, Bell C, Whyte T, Cardinal J, Macfarlane D, Rose S. Blood-brain barrier dysfunction following traumatic brain injury: correlation of K^{trans} (DCE-MRI) and SUVR (99mTc-DTPA SPECT) but not serum S100B. *Neurol Res* 2015;37:599-606
32. Heye AK, Thrippleton MJ, Armitage PA, Valdés Hernández M del C, Makin SD, Glatz A, et al. Tracer kinetic modelling for DCE-MRI quantification of subtle blood-brain barrier permeability. *Neuroimage* 2016;125:446-455
33. Payne-James J, Byard RW. *Encyclopedia of forensic and legal medicine*, 2nd ed. Oxford: Elsevier Ltd., 2015
34. Todd NV, Graham DI. Blood-brain barrier damage in traumatic brain contusions. *Acta Neurochir Suppl (Wien)* 1990;51:296-299
35. Albaugh MD, Orr C, Nickerson JP, Zweber C, Slauterbeck JR, Hipko S, et al. Postconcussion symptoms are associated with cerebral cortical thickness in healthy collegiate and preparatory school ice hockey players. *J Pediatr* 2015;166:394-400.e1
36. Benson RR, Meda SA, Vasudevan S, Kou Z, Govindarajan KA, Hanks RA, et al. Global white matter analysis of diffusion tensor images is predictive of injury severity in traumatic brain injury. *J Neurotrauma* 2007;24:446-459
37. Rutgers DR, Toulgoat F, Cazejust J, Fillard P, Lasjaunias P, Ducreux D. White matter abnormalities in mild traumatic brain injury: a diffusion tensor imaging study. *AJNR Am J Neuroradiol* 2008;29:514-519
38. Cohen BA, Inglese M, Rusinek H, Babb JS, Grossman RI, Gonen O. Proton MR spectroscopy and MRI-volumetry in mild traumatic brain injury. *AJNR Am J Neuroradiol* 2007;28:907-913

https://doi.org/10.3348/kjr.2020.0016